

# Hydrodynamic Characteristics of a New Sewer Overflow Screening Device: CFD Modeling & Analytical Study

M. A. Aziz, M. A. Imteaz, J. Naser, D. I. Phillips

**Abstract**—Some of the major concerns regarding sewer overflows to receiving water bodies include serious environmental, aesthetic and public health problems. A noble self-cleansing sewer overflow screening device having a sewer overflow chamber, a rectangular tank and a slotted ogee weir to capture the gross pollutants has been investigated. Computational Fluid Dynamics (CFD) techniques are used to simulate the flow phenomena with two different inlet orientations; parallel and perpendicular to the weir direction. CFD simulation results are compared with analytical results. Numerical results show that the flow is not uniform (across the width of the inclined surface) near the top of the inclined surface. The flow becomes uniform near the bottom of the inclined surface, with significant increase of shear stress. The simulation results promises for an effective and efficient self-cleansing sewer overflow screening device by comparing hydrodynamic results.

**Keywords**—Hydrodynamic Characteristics, Ogee Spillway, Screening, Sewer Overflow Device.

## I. INTRODUCTION

**D**URING wet weather conditions, sewer overflows to receiving water bodies raise serious environmental, aesthetic and public health concerns. To address these problems, different types of screening devices are used. Screening is a process that desirably is confined within the sewer system and automated in order to ensure operational safety. Floatable control is preferred by most of the proposed and existing environmental regulations. This requirement triggers the need to research the different types of screening devices and screenings handling systems to select the most appropriate for a particular installation especially at unmanned locations.

There are a number of different screening systems used in sewer overflow devices. One of the most used in practice is the rotary screen [20] which consists of a large rotating drum that is slightly angled to maximize dewatering. The angle of the drum ensures effective dewatering as the screenings travel up to the drum where they are removed from the unit. Reference [19] proposed a centrifugal screen having a series of screens attached to a cage that rotates around a vertical axis and where the flow enters from the bottom and flows upward to a deflection plate at the top of the unit and is collected from

outside the cage. Other types include disc types that consist of a flat disk covered with a screening media that rotates about a horizontal axis. The solids are retained by the screening media while the influent enters the submerged portion of the disc. A cleansing brush mechanism known as a brush raked fine screen is mounted on a drive shaft that slowly rotates in a 360 degree circle. In addition to these [20] an inclined static screen that acted as a sieve to remove solids from the liquid stream. On an overflow sewer screening device, a weir screen acts as a barrier to retain floatable and other solids and is cleaned by a rotating brush that is powered by the energy of water flowing over a water wheel or by an electric motor.

Some of the common drawbacks in the available commercial devices include inadequate screening capacity, external power needs and high cost [21]. Reference [17] showed a sewer overflow screening device with temporary holding tanks that provide transient storage and real time control of sewer systems. The device has no moving parts and has a robust stop/start operation, an effective self-cleansing mechanism resulting in low maintenance costs. It can be mounted downstream of the main overflow discharge weir. The hydraulic characteristics are very important in the effective functioning of such a self-cleansing screening device. The present study investigates the hydrodynamic characteristics of the new sewer overflow screening device that has a rectangular tank and an ogee weir to capture the gross pollutants. No external power source with mechanical or electrical components is needed for this self-cleansing device. This ogee weir mounted sewer overflow screening device works under extreme sewer overflow events with minimal inspection and maintenance needs.

The ogee weir spillway possesses excellent hydraulic features in terms of flow efficiency and relatively good flow measuring capabilities. In the studied device the differences from traditional weir flow considers upstream flow conditions, reflection waves due to short device boundary and shape and size change the flow properties. These slight changes need to be thoroughly researched to identify whether there are any detrimental effects to the evaluation of the performance of the spillway. Considerable researches have been carried out to determine the standard shape and size of the crest of the overflow spillway, relative height and upstream face slope of the spillway [12], [5]. Similar objectives have also been reported in the works of U.S. Army Corp of Engineers [16], [8]. Most of the previous investigations were confined to physical models. In recent years, with the advent of powerful

M. A. Aziz, M.A. Imteaz and J. Naser are with the Swinburne University of Technology, Faculty of Engineering and Industrial Science, Hawthorn, Victoria-3122, Australia (Phone: 61-03-9214-8160; fax: 61 3 9214 8264; e-mail: aaziz@swin.edu.au).

D. I. Phillips Author is with the Water Solutions Pty Ltd., Heathmont, Melbourne, Victoria 3135, Australia.

computational advances, research is focused on flow simulation using numerical modeling. An early attempt to model the spill overflow was done by [4] where it used potential flow theory and found good agreement with limited experimental data. Better accuracy with experimental data was found in the works of [10], [2] using linear finite element approximation. In addition 2D irrotational gravity flow over the curved water surface was successfully modeled [11], [9] expanded on the potential flow theory by applying an analytical functional boundary. 2D finite volume based numerical model for flow over spillway was validated using water level and pressure data on the physical model [13]. Some other important works include [3], [14] turbulence modeling and [15], [22] self-cleansing approach. Most of the existing literature reported either experimental works or numerically simulated flow phenomena over an ogee weir considering ideal conditions with no wave reflections and much bigger upstream and downstream boundaries. Although such assumptions simplify the problem they cannot be incorporated in the existing sewer drainage system, where space constrains for urban drainage system it would be a major issue.

As the proposed sewer overflow screening device is relatively small and wall reflection effects cannot be avoided, impacts of reflections on spillway flow characteristics need to be studied. This paper presents CFD simulated hydrodynamic characteristics of reflected sewer overflow on the weir and a comparison of such flow characteristics with one-dimensional analytical solutions.

## II. SCREENING MECHANISM

This proposed overflow sewer device will be installed downstream of an existing sewer overflow location. Fig. 1 shows the overflow sewerage device in the 1<sup>st</sup> phase. As sewage builds up in the left chamber (A), water pressure will push the floatable ball upward in the right chamber (B), which is connected to the left chamber via a pipe (C).

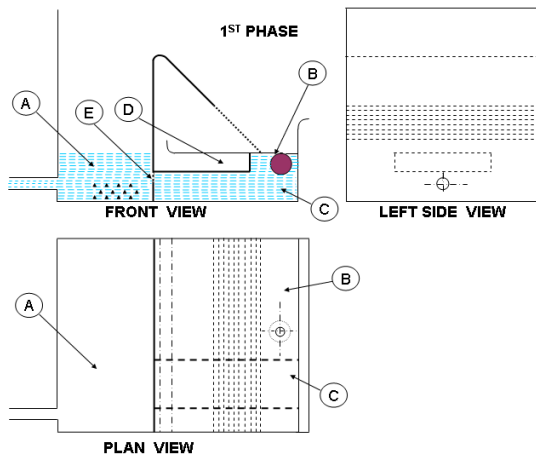


Fig. 1 Working diagram of the Sewer Overflow device

As the floatable ball goes upward, it will block the hole on the upper surface. It also shows the plan view of the proposed

device, showing the left and right box chambers and the vertical dotted lines (right) representing the screening device. The thick horizontal dotted lines represent the pipe connected the left and right chambers. The thick circle is the hole at the bottom of right chamber (B) and the dotted circle is the floatable ball.

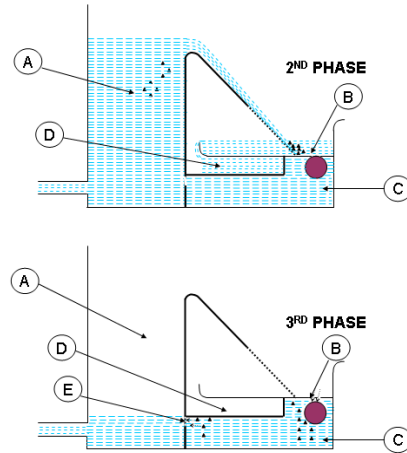


Fig. 2 Ogee weir is used to overflow the sewer water and pollutants are trapped in point B. Floating valve is open and pollutants are again return back to the system

The sewage builds up in the left chamber (A) until it becomes full, at which time the sewage will overflow the weir type structure. Fig. 2 shows the second phase of the scenario with the overflowing sewage. Towards the bottom of the sloping weir, the screen will exclude the solids while allowing the water to pass through the screen, bypassing the right chamber (B) and then to exit to the creek or waterway through two bypass channels (D). It also shows the third phase of the scenario, when the flow has subsided and the sewage level in the left chamber (A) is receding. Once the sewage level drops down to a certain level, the buoyancy pressure on the ball will reduce and the ball will drop, allowing the trapped pollutants to exit into the right chamber (through the pipe 'C') and then be flushed back into the sewer system.

## III. ANALYTICAL SOLUTION

To find an analytical solution using the Navier-Stokes equations some simple assumptions are made. Firstly, the flow is considered to be steady and uniform, flowing under the influence of gravity and parallel to the surface bottom while the effect of air viscosity at the free surface is negligible.

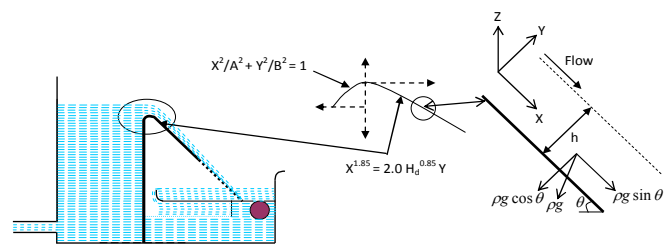


Fig. 3 Ogee weir design curve

As the surface is inclined we have to consider the body force. Therefore with constant viscosity Navier Stokes Equation becomes

$$\rho\left(\frac{\partial u}{\partial t} + u\frac{\partial u}{\partial x} + v\frac{\partial u}{\partial y}\right) = -\frac{\partial P}{\partial x} + \rho g_x + \mu\left(\frac{\partial^2 u}{\partial x^2} + \frac{\partial^2 u}{\partial y^2}\right) \quad (1)$$

$$\rho\left(\frac{\partial v}{\partial t} + u\frac{\partial v}{\partial x} + v\frac{\partial v}{\partial y}\right) = -\frac{\partial P}{\partial y} + \rho g_y + \mu\left(\frac{\partial^2 v}{\partial x^2} + \frac{\partial^2 v}{\partial y^2}\right) \quad (2)$$

The variables u, v, and w represent the velocities in the x-, y-, and z-directions;  $\rho$  = density;  $\mu$  = dynamic viscosity of water; P = defined as pressure;  $g_x, g_y$  are gravitational force in x and y directions. As we consider 1D flow the Z-direction need not to be considered and as the flow is steady  $\delta/\delta t = 0$ . Moreover the flow is parallel to the inclined surface, i.e. X-axis, so  $\delta u_x/\delta x = 0$  and  $u=0$ . As the flow is uniform the flow takes over a constant depth 'h' which leads pressure gradient  $\delta P/\delta x = 0$ . If 'Z' is the vertical direction, the potential per unit mass due to body force is  $g_z$ . Therefore the components of body force in X and Y directions are:

$$X = -\frac{\partial g_z}{\partial x} = -g\frac{\partial z}{\partial x} = g \sin \theta \quad (3)$$

$$Y = -\frac{\partial g_z}{\partial y} = -g\frac{\partial z}{\partial y} = -g \cos \theta \quad (4)$$

After incorporating all assumptions and components of body forces (1) and (2) reduces to:

$$g \sin \theta + v\frac{d^2 u}{dy^2} = 0 \quad (5)$$

$$-g \cos \theta - \frac{1}{\rho}\frac{\partial P}{\partial y} = 0 \quad (6)$$

From (6)

$$\delta P/\delta y = -\rho g \cos \theta$$

that leads to

$$P = -\rho g y \cos \theta + C \quad (7)$$

at  $y=h$ ,  $P=0$  atmospheric pressure i.e.  $C = \rho gh$

Therefore expression for pressure becomes,

$$P = \rho g \cos \theta (h - y) \quad (8)$$

Now integrating (5) twice with respect to y yields,

$$u_x = -\frac{g}{\nu} \sin \theta \frac{y^2}{2} + C_1 y + C_2 \quad (9)$$

At boundary condition  $y=0$ ,  $u_x=0$  i.e.  $C_2=0$ ; again at

$$y=h, \frac{du_x}{dy}=0; C_1 = g h \sin \theta / \nu;$$

$$u_x = \frac{\rho g}{2\mu} \sin \theta (2hy - y^2) \quad (10)$$

To get the shear stress at the boundary, applying Newton's law of viscosity-

$$\tau_{xy} = \mu \left. \frac{du_x}{dy} \right|_{y=0} = \mu \left\{ g \frac{\sin \theta}{\nu} (h - y) \right\}_{y=0},$$

which gives

$$\tau_{xy} = \rho g h \sin \theta \quad (\text{as } y=0) \quad (11)$$

q is the flow per unit width,

$$q = \int_0^h u_x dy = \int_0^h \frac{\rho g}{2\mu} \sin \theta (2hy - y^2) dy = \frac{1}{3\mu} \rho g h^3 \sin \theta \quad (12)$$

and average velocity,

$$v = \frac{q}{h} = \frac{1}{3\mu} \rho g h^2 \sin \theta \quad (13)$$

In the above equations, substituting inflow and weir surface angle with the horizontal, unit width of the weir, different hydrodynamic parameters were calculated. Reference [6] had developed standard shapes for downstream profile of the ogee weir defined by equation,

$$X^{1.85} = 2.0 H_d^{0.85} Y \quad (14)$$

The depth of water upstream of the spillway  $H_d$  is calculated from the non-dimensional equation for discharge given by,

$$Q = \frac{2}{3} C_0 \sqrt{2g} L H_e^{3/2} \quad (15)$$

where, Q = total discharge; L = Lateral crest length or Width;  $H_e$  = total head upstream from the crest; g = gravitational constant; and  $C_0$  = discharge coefficient. As the velocity head is relatively very small with total head  $H_d$  is consider equal with  $H_e$  which is 7.16 cm (that is,  $h/H_d$  greater than 1.33 and  $H_e = H_d$ , for the approach velocity head is negligible [5]. Moreover the effect of slope or roughness did not change the average value of  $H_e$  [7]. The curve of the ogee weir surface is drawn from the equation

$$Y = 1.744 X^{1.85} \quad (16)$$

The position (0, 39.5) is the starting coordinate over the ogee weir and different parameters are calculated based on different points are taken on the curve. The slope angles are used to calculate the analytical results for velocity, water level and shear stresses.

#### IV. CFD MODELING

The hydrodynamic characteristics of the overflow sewer screening device were investigated using state of art CFD modeling. A 3D numerical model was developed using commercially available CFD software AVL Fire [1] used in order to predict the flow over the ogee weir.

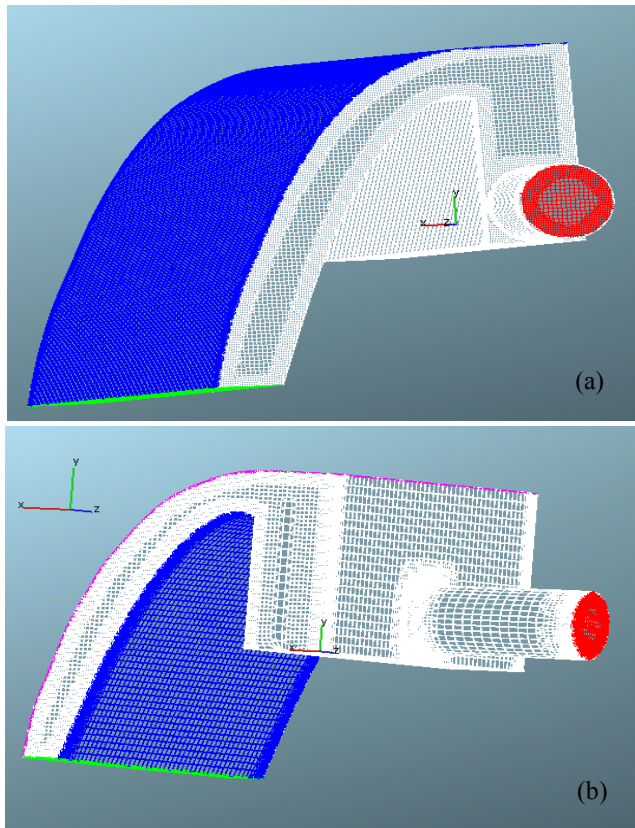


Fig. 3 Position 1(a) is the inlet parallel and Position 2 (b) is the inlet perpendicular to weir direction

The CFD software use finite volume method to solve the governing equations such as continuity, momentum and turbulence equations. The screening device has a rectangular tank (1m X 0.2m), an ogee weir and an inclined surface. The height of ogee weir bottom is 0.75m and the diameter of the inlet pipe is 0.2m. A design flow rate of 40 l/s was considered for the studied case. The outflow was assumed as free flow and perpendicular to outlet surface at the edge of weir. Two different inlet positions as shown in Fig. 3 were chosen to analyze below.

The model was simulated for a period of 180 seconds with a computational time step of 0.05 second. The results of the final time step are shown in the Fig. 4. A multiphase modeling approach was selected to model the air and water. Volume fraction of the water as phase 2 was selected to determine the free surface profile.

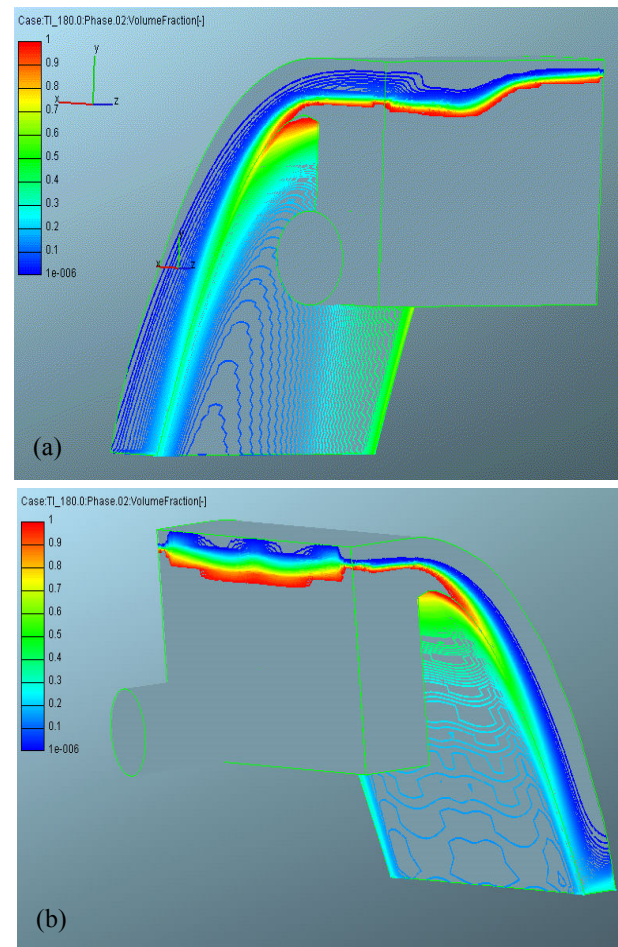


Fig. 4 Volume fraction of water for condition 1 (a) and Position 2 (b)

A color scale contour was used to differentiate air and water with scale 1 (red) as water and scale 1e-006 (blue) as air. The total number of cells for Position 1 was 27659 cells and for Position 2 were 38619 cells. The results of the final time steps volume fraction are shown in Fig. 4. In determining water level, assumptions were made based on the flooding and drying concept reported by [18], which refer that the value equal or over 50% of the volume fraction is considered as water level. Flow reflection is dominating over the cross section profile of the sewer overflow device. While analyzing the 3D numerical results for water level and velocities three distinct sections across the width of the weir were selected left, middle and right to show changing profiles. The position of left, middle and right in the simulation result are shown in Fig. 5. The first set over the weir, and the second and third sets, are 3cm and 6cm downstream of the ogee weir respectively. For parallel to the weir inlet data are consider as point 1, 2, 3 where as perpendicular to the weir inlet data are numbered as point 4, 5, 6 while analyzing numerical results.

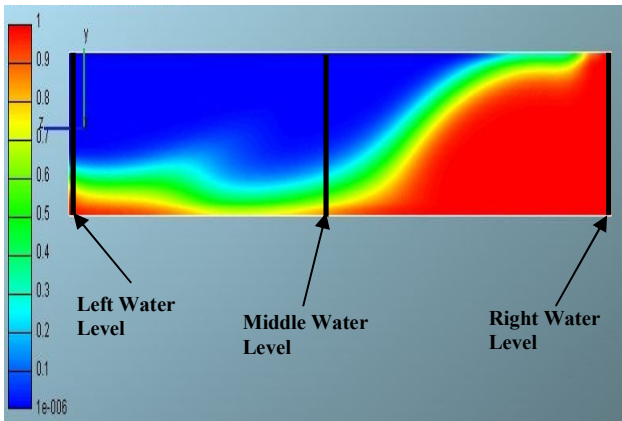


Fig. 5 Numerical results of water level over ogee weir showing different position

#### V. DISCUSSION OF HYDRODYNAMIC RESULTS

To understand flow reflections, CFD simulated water levels at left, middle and right sections along the flow were extracted. These results were compared with the one-dimensional analytical solution considering steady, incompressible fluid. Analytical formulation is unable to include flow reflections from the wall. A model result shows the dominant effect of flow reflection in the relatively small sewer overflow device as shown in Fig. 5. The CFD simulated results show that due to flow reflection under condition1 (inlet parallel to the weir), water level at right side is overriding the water levels at middle and left sections. Whereas, under condition2 (inlet perpendicular to the weir), reflected flow contributes to elevated water levels towards both the left and right sides of the device, as shown in Fig. 6.

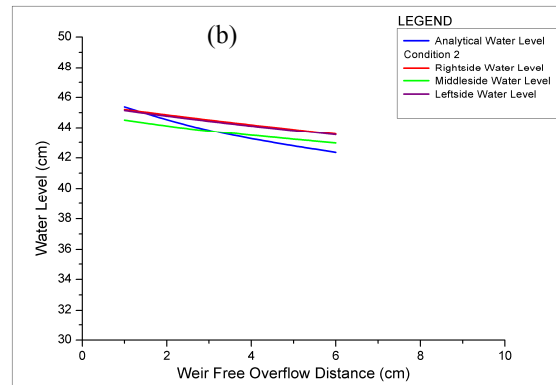
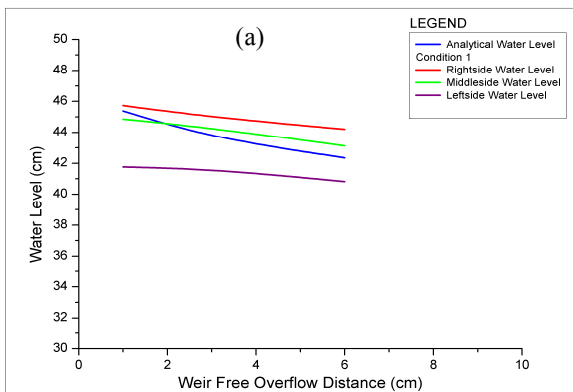


Fig. 6 Comparison of water level along the flow for Position 1(a) and 2(b)

However towards the bottom of the inclined surface, the flow becomes uniform (across the width). The reflected water level in the right side reduces as the flow travels downstream of the ogee weir (condition 1).

Fig. 7 shows how the velocity changes over the weir. As the flow propagates downstream of the weir, the velocity at the bottom increases three times the velocity over the ogee weir in both cases, that will effectively increase the self-cleansing capacity of the device.

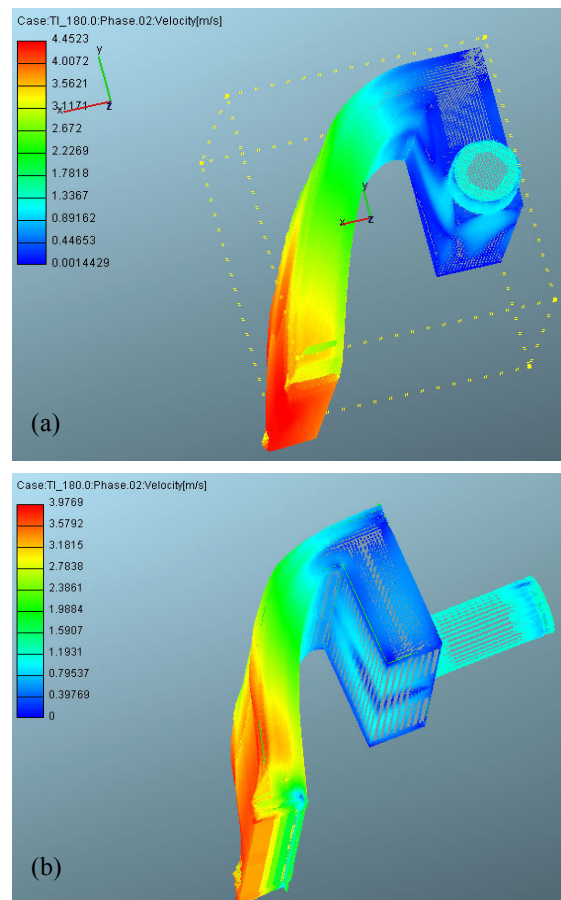


Fig. 7 Velocity vector at parallel (a) and perpendicular (b) inlet to the weir directions

The comparisons for velocity, water level and shearing stress are shown in the table below.

TABLE I  
 CALCULATION OF DIFFERENT PARAMETERS

| Inlet Parallel to Ogee Weir |          |       |                       |        |       |                                  |        |       |            |                           |        |       |                                 |        |       |       |       |
|-----------------------------|----------|-------|-----------------------|--------|-------|----------------------------------|--------|-------|------------|---------------------------|--------|-------|---------------------------------|--------|-------|-------|-------|
| Above the Weir (m)          | Location | Point | Water Level Numerical |        |       | Average Velocity (m/s) Numerical |        |       | Analytical | Volume Fraction Numerical |        |       | Shear Stress (N/sq m) Numerical |        |       |       |       |
|                             |          |       | Left                  | Middle | Right | Left                             | Middle | Right |            | Left                      | Middle | Right | Left                            | Middle | Right |       |       |
|                             | X=0.005  | 1     | 2.26                  | 5.35   | 6.23  | 5.88                             | 0.38   | 0.61  | 0.51       | 0.59                      | 0.54   | 0.63  | 0.54                            | 29.91  | 16.19 | 13.48 | 24.77 |
|                             | X=0.030  | 2     | 2.32                  | 4.97   | 5.67  | 4.33                             | 0.56   | 0.8   | 0.7        | 0.79                      | 0.5    | 0.57  | 0.6                             | 54.97  | 22.51 | 14.49 | 36.52 |
|                             | X=0.060  | 3     | 2.04                  | 4.34   | 5.42  | 3.57                             | 0.76   | 0.96  | 0.95       | 0.96                      | 0.52   | 0.58  | 0.64                            | 81.07  | 30.32 | 11.61 | 37.53 |

| Inlet Perpendicular to Ogee Weir |          |       |                       |        |       |                                  |        |       |            |                           |        |       |                                 |        |       |       |       |
|----------------------------------|----------|-------|-----------------------|--------|-------|----------------------------------|--------|-------|------------|---------------------------|--------|-------|---------------------------------|--------|-------|-------|-------|
| Above the Weir (m)               | Location | Point | Water Level Numerical |        |       | Average Velocity (m/s) Numerical |        |       | Analytical | Volume Fraction Numerical |        |       | Shear Stress (N/sq m) Numerical |        |       |       |       |
|                                  |          |       | Left                  | Middle | Right | Left                             | Middle | Right |            | Left                      | Middle | Right | Left                            | Middle | Right |       |       |
|                                  | X=0.005  | 4     | 5.64                  | 5.01   | 5.71  | 5.88                             | 0.52   | 0.63  | 0.53       | 0.59                      | 0.58   | 0.53  | 0.57                            | 29.91  | 44.55 | 10.04 | 36.8  |
|                                  | X=0.030  | 5     | 5.08                  | 4.4    | 5.19  | 4.33                             | 0.67   | 0.83  | 0.68       | 0.79                      | 0.56   | 0.57  | 0.54                            | 54.97  | 44.8  | 12.34 | 35.86 |
|                                  | X=0.060  | 6     | 4.73                  | 4.19   | 4.78  | 3.57                             | 0.85   | 0.99  | 0.86       | 0.96                      | 0.56   | 0.54  | 0.56                            | 81.07  | 48.24 | 13.47 | 35.95 |

Fig. 8 shows the comparison of shearing stress near the ogee weir. CFD simulation shows formation of flow separation near the ogee weir. The CFD simulated shear stress is lower than the analytical value as it is unable to consider flow undulations. Moreover analytical calculation assumed an in-viscid fluid domain without having any boundary layer effect while CFD simulation considered viscous boundary effects. Analysis of the shear stress along the flow path was performed to identify efficient self-cleansing screeners. From CFD simulation it was shown that the shear stress increases significantly towards the bottom of the inclined surface, which suggests that, the location of screen should be towards the bottom. Moreover, the flow becomes uniform across the width in this area, which will also help effective screening.

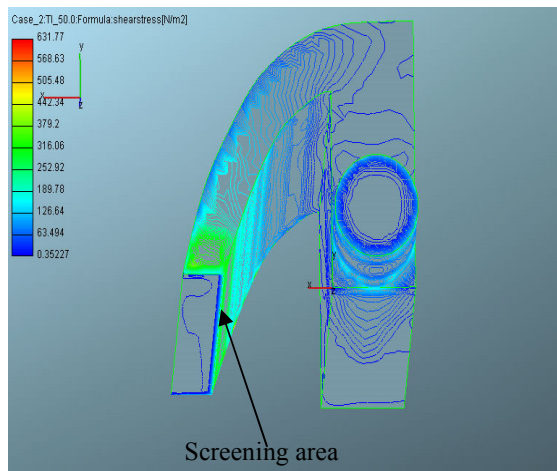


Fig. 8 Shear stress distribution at parallel inlet to weir directions

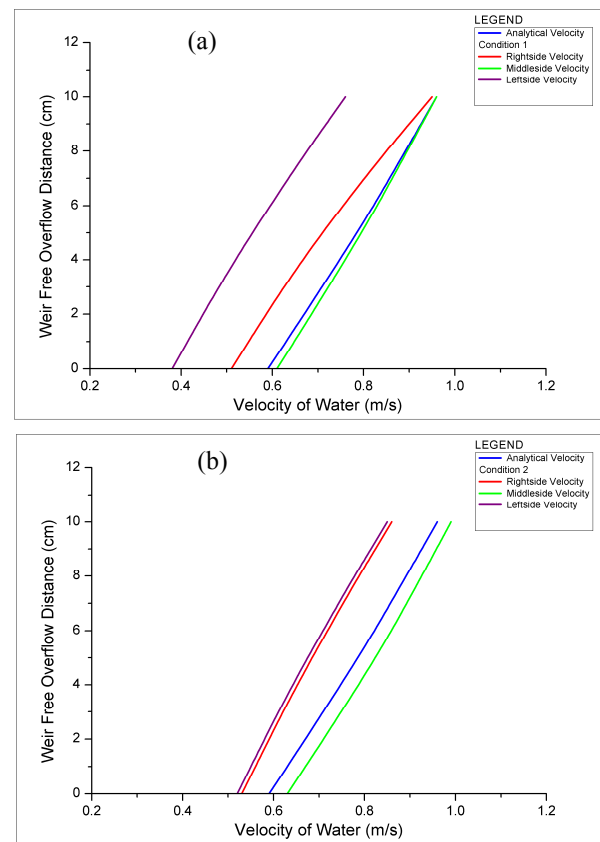


Fig. 9 Comparison of flow velocities along the width for Position 1 (a) and 2 (b)

To understand how the velocities change due to the reflection effect at different sections, comparison of velocities at different inlet orientations are shown as 'Position 1 (a)' and 'Position 2 (b)'.

As the water flows down, its velocity increases due to gravitational acceleration as shown in Fig. 9. Due to varying water levels (high water level near the right side and low water level near the left side), near the top of the weir surface, the self-cleansing property will not be as effective near the top region at condition1. If screens are provided near the top of the weir

surface at condition1, only the right-hand side strip will get efficient self-cleansing while the left side holes are likely to be blocked by larger pollutants in the sewer water. However as flow becomes uniform (across the width) near the bottom of the weir surface, the self-cleansing capability can be achieved. Keeping this fact in mind, it is proposed to provide perforations (circular holes) near the bottom of the weir surface. These phenomena will be verified through further experimental study of this device.

## VI. CONCLUSIONS

A 3D Computational Fluid Dynamics model was developed for a proposed sewer overflow screening device. Model simulated flow behaviors on the inclined surface of the device showed where perforations should be provided for best trapping of the gross pollutants from sewer overflows. As the device is to have a self-cleansing capability from the flow itself, the flow pattern on the inclined surface is important. As the sewer overflow device is small, the reflection effect was found to be dominant in the numerical results. Numerical results show that the flow is not uniform (across the width of the inclined surface) near the top of the inclined surface due to the flow reflections by the rectangular box wall of the device. However, the flow becomes uniform near the bottom of the inclined surface, with significant amount of shear stress. This suggests that the perforations should be placed near the bottom of the inclined surface to achieve an effective self-cleansing capability for the device. Uniform flow towards the bottom of the inclined surface will help to remove any pollutants adhered to the perforations. An analytical solution for the flow over the inclined surface was derived for one-dimensional flow. CFD results were compared with the one-dimensional analytical results for different flow parameters. The one-dimensional analytical solution was unable to produce three-dimensional flow reflection effects. Discrepancies with numerical results have been discussed. It is recommended that analytical solutions be performed for a two dimensional case and compared the numerical results from the two-dimensional analytical solution. A series of laboratory experiments will be conducted with different testing conditions and the CFD simulated results will be evaluated by comparison with the results of the laboratory experiments.

## REFERENCES

- [1] AVL Fire CFD Solver v8.5 manual, 2008, A-8020 Gras, Austria, [www.avl.com](http://www.avl.com).
- [2] P. L. Betts, "A variation principle in terms of stream function for free surface flows and its application to finite element method", *Comp. and Fluids*, Vol.7(2), 1979, pp.145-153.
- [3] M. F. Burgisser, and P. Rutschmann, "Numerical solution of viscous 2DV free surface flows: Flow over spillway crests", *Proc.*, 28<sup>th</sup> IAHR Congr., Technical University Graz, Graz, Austria, 1999.
- [4] J. J. Cassidy, "Irrotational flow over spillways of finite height", *J. Engrg. Mech. Div.*, ASCE, Vol. 91(6), pp.155-173, 1965.
- [5] V. T. Chow, *Open-channel hydraulics*, McGraw-Hill, New York, pp.365-380, 1959.
- [6] U.S. Army Corps of Engineers. "Corps of Engineers Hydraulic Design Criteria", prepared for office of the chief of engineers, Waterways Experiment Station, Vicksburg, Miss, 1952.

- [7] D.A. Kraijenhoff, and A. Dommerholt, "Brink depth method in rectangular channel", *Journal of Irrigation and Drainage Division ASCE* 103 (2) pp.171-177, 1977.
- [8] U.S. Bureau of Reclamation. "Design of small dams", U.S. Government Printing Office, Washington, D.C, 1977.
- [9] Y. Guo, X. Wen, C. Wu, and D. Fang, "Numerical modelling of spillway flow with free drop and initially unknown discharge", *J. Hydr. Res.*, Delft, The Netherlands, Vol. 36(5), pp. 785-801, 1998.
- [10] M. Ikegawa, and K. Washizu, "Finite element method applied to analysis of flow over a spillway crest", *International Journal of Numerical Methods in Engineering*, 6, pp. 179-189, 1973.
- [11] W. Li, Q. Xie, and C. J. Chen, "Finite analytic solution of flow over spillways", *J. Engrg. Mech.*, ASCE, 115(12), pp. 2635-2648, 1989.
- [12] S. T. Maynard, "General spillway investigation", *Tech. Rep. HL-85-1*, U.S. Army Engineer Waterways Experiment Station, Vicksburg, Miss, 1985.
- [13] M. R. Bhajantri, T. I. Eldho, P. B. Deolalikar, "Hydrodynamic modelling of flow over a spillway using a two-dimensional finite volume-based numerical model", *Sadhana* Vol. 31, Part 6, December, pp. 743-754, 2006.
- [14] N. R. Olsen, and H. M. Kjellesvig, "Three-dimensional numerical flow modelling for estimation of spillway capacity", *J. Hydr. Res.*, Delft, The Netherlands, Vol. 36(5), pp. 775-784, 1998.
- [15] D. I. Phillips, and M. Simon, "A sewage solids screening system for CSO chambers. Novatech 2007", *Proc 6<sup>th</sup> International Conference, Sustainable techniques and Strategies in Urban Water Management*, Lyon, France, Vol 2, pp. 697-704, 2007.
- [16] U.S. Army Corp of Engineers. "Hydraulic design of spillways", EM 1110-2-1603, Dept. of the Army, Washington, D.C., 1990.
- [17] M. Simon, and D. I. Phillips, "The development of a sewer solids screening system for CSO chambers", *Proceedings of the 11<sup>th</sup> International Conference on Urban Drainage*, Edinburgh, Scotland, UK, 2008.
- [18] G. S. Stelling, "On the construction of computational methods for shallow water equations", *Rijkswaterstaat communication* No. 35/1984
- [19] Metcalf and Eddy, *Wastewater Engineering, Treatment, Disposal and Reuse*, Third Ed., Boston, MA: McGraw-Hill, Inc. pp. 448-451, 1991.
- [20] P. E. Moffa, *Scarborough CSO Project-Review of CSO Screen Application*, report prepared for the City of Scarborough, Municipality of Metro, Toronto, ON, 1997.
- [21] M. Simon, Vorthbach km 2+335 bis 3+500 *Hydraulische Bestandsuntersuchung und Vorschlag zur Veränderung*. Report prepared for the Emschergenossenschaft, Essen, Germany, 2003.
- [22] Aziz, M.A., Imteaz, M.A., Choudhury, T.A., and Phillips, D.I., "Artificial Neural Networks for the prediction of the trapping efficiency of a new sewer overflow screening device", *19th International Congress on Modelling and Simulation*, Perth, Australia, 2011.